PCCP

PAPER

View Article Online
View Journal | View Issue

Cite this: *Phys. Chem. Chem. Phys.*, 2016, **18**, 11821

Electron conjugation *versus* π–π repulsion in substituted benzenes: why the carbon–nitrogen bond in nitrobenzene is longer than in aniline

Huaiyu Zhang,[ab] Xiaoyu Jiang,[c] Wei Wu[a] and Yirong Mo*[b]

Received 21st January 2016,
Accepted 25th January 2016

DOI: 10.1039/c6cp00471g

www.rsc.org/pccp

Gas-phase electron diffraction experiments show that the C–N bond in aniline (1.407 Å) is significantly shorter than in nitrobenzene (1.486 Å). It is known that the amino group is electron-donating and the nitro group is electron-withdrawing, and both substitution groups can effectively conjugate with benzene. Thus, it is puzzling why the C–N bond in nitrobenzene is even longer than the single C–N bond in methylamine (1.472 Å). In this work, we performed computations by strictly localizing the π electrons with the block-localized wavefunction (BLW) method, which is a variant of *ab initio* valence bond theory. Geometry optimizations of electron-localized states, where the conjugation over the C–N bond is quenched, show that the conjugation in nitrobenzene is only half of the conjugation in aniline. But even in optimal electron-localized states, the C–N bond in nitrobenzene is still 0.074 Å longer than in aniline. As a consequence, it is indeed not the π conjugation which is responsible for the disparity of the C–N bond distances in these systems. Instead, we demonstrated that the π–π repulsion, which is contributed by both Pauli exchange and electrostatic interaction, plays the key role in this "abnormal" behavior. Notably, the π resonance within the nitro group generates a considerable dipole, which repels the π electrons in the benzene ring. The deactivation of the resonance within the nitro group significantly shortens the C–N bond by 0.06 Å. The unfavorable π–π electrostatic repulsion is further exemplified by N_2O_4. In fact, the destabilizing π–π repulsion is ubiquitous but largely neglected in conjugated systems where only the stabilizing conjugation is the focus. Experimental phenomena such as the C–N bond distances in aniline and nitrobenzene result from the balance of both stabilizing and destabilizing forces.

1. Introduction

Conjugation is one of the landmark concepts in chemistry, and has been associated with the high stability, planarity, small bond length alternation and many other physicochemical properties such as the bathochromic shift and the lifetime of excited states in conjugated systems. From the viewpoint of molecular orbital (MO) theory, conjugation occurs from an occupied orbital in one moiety (such as a double or triple bond) to the other moiety's virtual orbital. Alternatively, valence bond (VB) theory illustrates conjugation in terms of resonating Lewis (or resonance) structures,[1] and conjugation (resonance) energy can be derived "by subtracting the actual energy of the molecule in question from that of the most stable contributing structure".[2] Thus, by definition, conjugation must be stabilizing. Cyclic conjugation leads to another prominent chemistry concept, aromaticity, as notably exemplified by benzene.[3–5] Aromaticity is originally measured as the extra cyclic conjugation stabilization in aromatic systems compared with corresponding noncyclic conjugated reference molecules.[6–10] But the difficulty in directly computing resonance energies leads to numerous indirect measures based on energetic, geometric, electronic, magnetic, and other spectroscopic (IR and UV) criteria which have been proposed to characterize aromaticity and antiaromaticity. Most of these measures rely on other references. One simple yet reliable approach with no need of references is the Nucleus-Independent Chemical Shift (NICS) probe proposed by Schleyer and coworkers.[11] NICS refers to the chemical shielding computed in or above ring centers.[12]

Chemists have been long intrigued by the influence of substituents on the properties and reactivity of benzene. For instance, an amino substituent remarkably increases the rate

[a] *The State Key Laboratory of Physical Chemistry of Solid Surfaces, iChEM, Fujian Provincial Key Laboratory of Theoretical and Computational Chemistry and College of Chemistry and Chemical Engineering, Xiamen University, Xiamen, Fujian 361005, China*
[b] *Department of Chemistry, Western Michigan University, Kalamazoo, Michigan 49008, USA. E-mail: ymo@wmich.edu*
[c] *College of Ecological Environment and Urban Construction, Fujian University of Technology, Fuzhou 350108, China*

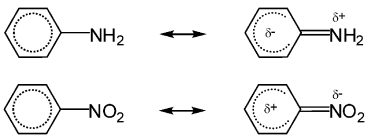

Scheme 1 Resonance structures of aniline and nitrobenzene within the two-state model.

of electrophilic substitution, while a nitro substituent decreases the benzene ring's reactivity significantly. The resonance between the benzene ring and its substituent is shown in Scheme 1.

In Scheme 1, the left resonance structures correspond to diabatic electron-localized states before any electron is delocalized between the benzene ring and a substituent, while the right ones are diabatic states with electrons already delocalized (transferred). Thus, the conjugation in aniline and nitrobenzene can be well studied within the electron transfer theory using a two-state model.[13–18] While conjugation between the benzene ring and a substituent stabilizes the system as a whole, the aromaticity within the benzene ring may be more or less reduced as the π-sextet rule[19,20] is slightly broken. This substituent effect has also been intuitively summarized by Hammett's substituent constant σ.[21] A negative σ indicates an electron donating nature of the substituent (*e.g.*, −0.66 at the *para* position of aniline), and a positive σ corresponds to an electron withdrawing nature of the substituent (*e.g.*, +0.778 at the *para* position of nitrobenzene). Obviously, the substituent constant is correlated with the molecular dipole moment. A further detailed analysis, however, shows that the influence of a substituent comes from two sources, namely the σ inductive effect and the π resonance (or mesomeric) effect.[22–25] While both amino and nitro exhibit similar inductive effect, they have contrast behaviors for their π conjugation capability. But no matter what the direction of electron movement is, the C–N bonds in both aniline and nitrobenzene are always of certain double bond properties. Thus, it draws our attention that the gas-phase electron diffraction experiments show a significant disparity for the C–N bond lengths between aniline (1.407 Å)[26] and nitrobenzene (1.486 Å).[27] For comparison, the C–N bonds in methylamine (1.472 Å[28]) and nitromethane (1.488 Å[29]) are comparable and close to the bond in nitrobenzene. As bond lengths generally correlate with bond energies,[30,31] the much longer bond length in nitrobenzene implies that the C–N bond is even weaker than the single C–N bond in methylamine.

Both aniline[32–41] and nitrobenzene[42–48] have been extensively studied in the literature. In aniline, the amino group is slightly pyramidal and the nitrogen is believed to take a hybridization mode between sp^3 and sp^2, due to the resonance interaction between the benzene ring and the nitrogen lone pair. The latter also results in a low inversion barrier (1–2 kcal mol^{-1}) for the amino group,[34,36] compared with 4–5 kcal mol^{-1} in aliphatic amines and 5.0 kcal mol^{-1} in ammonia.[49] In contrast, in nitrobenzene the nitrogen adopts a planar sp^2 hybridization mode and thus there is no inversion barrier. In general, it is well recognized that the increasing s component in a hybrid orbital leads to a shorter bond, as observed in C–H bond lengths in ethane (1.096 Å), ethene (1.085 Å), and ethyne (1.061 Å).[50] Thus, the much shorter C–N bond in aniline than in nitrobenzene is puzzling.

To probe the origin of the disparity in aniline and nitrobenzene and differentiate the σ inductive effect and the π resonance, it is essential to get the optimal bond lengths when the conjugation over C–N bonds in these systems is hypothetically and completely quenched. But in MO theory, all orbitals are expanded over the whole system and thus delocalized. Numerous post-SCF localization schemes have been proposed, but all these schemes simply reshuffle canonical MOs and project localized orbitals from delocalized MOs. While the resulting localized orbitals are illustrative and physically meaningful, they are not optimal and thus quantitatively could be misleading, let alone the optimal electron-localized geometries which are not available from any MO-based method. Different from but complementary to the routine MO or DFT methods, VB theory starts from local orbitals to construct Lewis structures in the form of Heitler–London–Slater–Pauling (HLSP) functions.[51–55] Among a number of *ab initio* VB approaches is the block-localized wavefunction (BLW) method which is the simplest and most efficient.[56–58] In the BLW method, we block-localize the molecular or Kohn–Sham orbitals and hence the associated electron density is constrained by construction. The uniqueness of the BLW is that it can easily generate optimal geometries for electron-localized states.[59]

In this work, we performed BLW studies of aniline and nitrobenzene, together with NICS computations, in order to elucidate the impact of substitution on aromaticity and the difference of the C–N bond lengths in these two systems. For comparison, benzene and dithionitrobenzene were also computed and analyzed.

2. Computational methods

Most computational tools are based on MO theory and use a top–down strategy, *i.e.*, derive optimal canonical MOs which are delocalized, then project out the bonding picture from delocalized MOs. Alternatively, the VB theory adopts a bottom-up way and constructs molecular wavefunctions with resonating Lewis structures built from localized bond orbitals which are self-consistently optimized. In VB theory, a Lewis structure for a system of $N = 2n + 2S$ electrons (S is the spin quantum number) is described with a HLSP function as

$$\Phi_K = M_K\hat{A}(\varphi_{1,2}\varphi_{3,4}\cdots\varphi_{2n-1,2n}\phi_{2n+1}\alpha(2n+1)\cdots\phi_N\alpha(N)) \quad (1)$$

where M_K is the normalization constant, $\hat{A}$ is the antisymmetrizer and $\varphi_{i,j}$ is a bond function corresponding to the bond between orbitals ϕ_i and ϕ_j (or a lone pair if $\phi_i = \phi_j$)

$$\varphi_{i,j} = \hat{A}\{\phi_i\phi_j[\alpha(i)\beta(j) - \beta(i)\alpha(j)]\} \quad (2)$$

In eqn (1) there are $2S$ singly occupied orbitals from ϕ_{2n+1} to ϕ_N. As each bond function can be expanded into 2 Slater determinants, a HLSP comprises of 2^n Slater determinants. The overall

many-electron wave function for a system is a linear superposition of VB functions

$$\Psi = \sum_K C_K \Phi_K \tag{3}$$

The computations of the Hamiltonian and overlap matrix elements between VB functions remain the major task for *ab initio* VB methods.[55] One way to significantly reduce the computational costs is the use of nonorthogonal doubly occupied bond orbitals which were late generalized to fragment-localized orbitals.[60–67] In the BLW method where a BLW corresponds to an electron-localized diabatic state,[56–58] it is assumed that the total electrons and primitive basis functions can be divided into several subgroups (blocks), and each MO φ_{ij} is block-localized and expanded in only one block i whose subspace is composed of m_i basis functions $\{\chi_{i\mu}\}$ as

$$\varphi_{ij} = \sum_{\mu=1}^{m_i} C_{ij\mu}\chi_{i\mu} \tag{4}$$

Subsequently, the BLW is defined using a Slater determinant and in the case of $S = 0$

$$\begin{aligned}\Psi^{\mathrm{BLW}} &= M \det\left|\varphi_{11}^{2}\varphi_{12}^{2}\cdots\varphi_{1\frac{n_1}{2}}^{2}\varphi_{21}^{2}\cdots\varphi_{i1}^{2}\cdots\varphi_{i\frac{n_i}{2}}^{2}\cdots\varphi_{k\frac{n_k}{2}}^{2}\right| \\ &= M\hat{A}[\Phi_1\cdots\Phi_i\cdots\Phi_k]\end{aligned} \tag{5}$$

where Φ_i is the direct product of block-localized orbitals in block i. Orbitals in the same subspace are subject to the orthogonality constraint, but orbitals belonging to different subspaces are nonorthogonal. Since Kohn–Sham DFT has a self-consistent procedure identical to the HF method except that the HF exchange potential is replaced by a DFT exchange–correlation (XC) potential, the BLW method can be straightforwardly extended to the DFT level.[58] The self-consistent optimization of orbitals can be accomplished using successive Jacobi rotation[57] or the algorithm by Gianinetti *et al.*[64,65] The latter generates coupled Roothaan-like equations and each equation corresponds to a block, thus is highly efficient. Whereas we can construct different BLW for different resonance structures and derive the final wavefunction with eqn (3), we understand that a delocalized wavefunction from the MO or DFT method is essentially a combination of all resonance structures. As such, the conjugation can be defined as the energy difference between a MO or DFT state and the BLW state as

$$\Delta E_{\mathrm{c}} = E(\Psi^{\mathrm{BLW}}) - E(\Psi^{\mathrm{DFT}}) \tag{6}$$

Since the BLW method can optimize the geometries of electron-localized states,[59] there are two types of resonance energies based on the geometries used in BLW computations. Adiabatic resonance energy (ARE) is defined as the energy difference when both BLW and DFT computations at their respective optimized geometries, whereas vertical resonance energy (VRE, or quantum mechanical resonance energy) is the energy difference between the BLW and DFT computations at the same DFT optimal geometry.

For aniline and nitrobenzene, our focus is on the π delocalization between benzene and substituents, and thus we partition all orbitals and electrons to two blocks, one is the six electrons on benzene, and the other includes all the remaining ones where σ and π orbitals will be naturally separated. In the case of rotating the nitro group in nitrobenzene, three blocks are needed to allow the separation of the π electrons on the nitro group from the σ frame. Standard B3LYP DFT calculations with the basis set of 6-311+G(d,p) were performed throughout the work. The principal resonance structures with six π electrons strictly localized on the benzene rings (left ones in Scheme 1) are obtained with the BLW method at the same DFT level, which has been implemented in our in-house version of the quantum mechanical software GAMESS.[68] The comparison of the geometrical parameters and molecular energies computed with the standard B3LYP and the BLW methods manifests the impact of the resonance between benzene and its substituents. NICS computations were performed with Gaussian09 at the same theoretical level.[69]

3. Results and discussion

DFT computations

We first performed geometry optimizations at the B3LYP/6-311+G(d,p) theoretical level, followed by the NICS analyses. The major findings are summarized in Table 1. It is obvious that the theoretical level used in this study can appropriately derive the geometries as the C–N bond lengths in aniline (1.399 Å) and nitrobenzene (1.481 Å) are very close to experimental data (1.407 Å[26] and 1.486 Å[27]). For comparison, methylamine has an optimal C–N bond distance of 1.465 Å, also close to the experimental value 1.472 Å.[28] Thus, computations verify that the C–N bond in nitrobenzene is indeed longer and weaker than the single C–N bond in methylamine. Due to the conjugation over the C–N bond and the subsequent reduction of the nitrogen lone pair and NH bonds, the amino group in aniline is highly flattened with the CNH bond angle 115.6° and the CCNH dihedral angle 24.5°.

As the six π electrons in benzene exhibit the perfect aromaticity, either removing or adding π electrons to the cycle would destroy the sextet,[19,20] leading to a reduction of the aromaticity. Here we use the NICS[11,12] as a measure of the aromaticity. Table 1 compares the NICS values in the ring centers of aniline and nitrobenzene with the values in benzene. While for aniline both NICS(0) and NICS(1) are reduced in comparison with benzene, nitrobenzene has enhanced NICS values, though the enhancement in NICS(1) is much weaker than in NICS(0). This seems

Table 1 Optimal C–N bond distances (Å), C–N bond dissociation energy (ΔE_{d} in kcal mol^{-1}) and NICS values for aniline and nitrobenzene compared with benzene from DFT computations at the B3LYP/6-311+G(d,p) level

Molecule	R(C–N)	ΔE_{d}	NICS(0)	NICS(1)	NICS$_{zz}$(0)	NICS$_{zz}$(1)
C_6H_5–NH_2	1.399	108.8	−7.82	−9.11	−9.84	−25.00
C_6H_5–NO_2	1.481	76.9	−9.02	−10.33	−13.02	−27.50
C_6H_6	—	—	−8.02	−10.10	−14.48	−29.23
C_6H_5–NS_2	1.472	72.2	−7.29	−9.29	−9.74	−25.13

different from our expectations. As the focus is on the out-of-plane tensor of shielding caused by the ring current, $NICS_{zz}$ has been proved to be a better indicator than NICS for aromaticity.[70] Table 1 does indicate that $NICS_{zz}(0)$ and $NICS_{zz}(1)$ are diminished in both aniline and nitrobenzene. Significantly, the reduction is much more significant in aniline than in nitrobenzene. Natural population analysis (NPA)[71] also shows that the π electron population in the ring increases to 6.143 e in aniline but decreases to 5.933 e in nitrobenzene. This may imply that the magnitude of conjugation in nitrobenzene is much less than in aniline.

BLW computations

By strictly localizing the six π electrons in the benzene ring and quenching the conjugation over the C–N bond, BLW geometry optimizations lead to much stretched C–N bond in both systems as shown in Table 2. The comparison between Tables 1 and 2 shows that conjugation shortens C–N bonds by 0.092 and 0.084 Å in aniline and nitrobenzene, respectively. These shortenings are quite close and in line with the strength of conjugation (see Table 2). Without conjugation, as expected, the pyramidality of the amino group in aniline would be very much like in ammonia, as the BLW optimization results in the CNH bond angle 108.7° and the dihedral angle 114.4°, compared with 107.9° and 116.4° for ammonia at the same level. One may wonder why the C–N single bond in aniline (1.491 Å) is a little longer than the bond length in methylamine (1.465 Å). The reason is that in the latter there is nonnegligible hyperconjugative interactions between the methyl and amino groups, very much like the hotly debated ethane case.[72–79] Although we believe that the ethane rotational barrier is largely caused by the steric repulsion, there is secondary $\sigma_{CH} \rightarrow \sigma_{CH}^*$ hyperconjugation which shortens the central C–C bond by 0.040 Å.[80] Thus, without hyperconjugation, the C–N bond would be also stretched a little bit in methylamine.

Energetically, as shown in Table 2, conjugation stabilizes both aniline and nitrobenzene, but the conjugative stabilization in aniline is almost twice as large as in nitrobenzene. To probe the orbital interactions in detail, we examined the orbital energy changes from block-localized to delocalized. Fig. 1 shows the "*in situ*" orbital interaction diagrams for aniline and nitrobenzene. We note that this kind of "*in situ*" diagram is remarkably different from those for intermolecular interactions which can be found in extensive literature. The often-seen orbital interaction diagram tries to establish the correlation between a complex and its separated, non-interactive monomers. But in the present "*in situ*" orbital diagram, all parts are put together just like in the complex, thus there are still physical or field (electrostatic) interactions among them, though the orbital interactions have been disabled. We believe that the present "*in situ*" orbital diagram derived from BLW computations is more insightful and informative than the regular ones.

Table 2 Optimal C–N bond distances (Å) and conjugation energies (kcal mol^{-1}) from BLW computations at the B3LYP/6-311+G(d,p) level

Molecule	R(C–N)	ΔE_c(TRE)	ΔE_c(ARE)
C_6H_5–NH_2	1.491	19.3	15.2
C_6H_5–NO_2	1.565	10.8	8.8
C_6H_5–NS_2	1.579	13.4	10.3

Fig. 1 shows that the HOMO of the amino group (*i.e.*, lone pair on nitrogen) and the LUMO of the benzene ring have an energy gap of 6.70 eV, but the involvement of the HOMO of benzene which has comparable energy with the HOMO of amino leads to significant stabilization of the delocalized HOMO−1 orbital in aniline, though the HOMO is pushed up a little. Overall the energy stabilization from the orbital interactions among the three block-localized orbitals is 0.72 eV, or 16.6 kcal mol^{-1}. This value is close to the ΔE_c(TRE) in Table 1. In contrast, although the energy difference between the HOMO of benzene and the LUMO of the nitro group is relatively low, 5.42 eV, their interaction seems less productive as the delocalized HOMO is only stabilized by 0.14 eV, or 3.2 kcal mol^{-1}. This indicates that the conjugative stabilization in nitrobenzene comes from the interaction among all orbitals, rather than dominated by a major mode as in aniline.

An alternative way to visualize the conjugation is the electron density difference (EDD) maps, which manifest the difference between the electron-localized state (BLW) and the electron-delocalized state (DFT) and thus reflect the movement of electron density. Fig. 2 shows plots of the EDD maps for aniline and nitrobenzene. The comparison of Fig. 2a and b reveals the dramatically different behaviors of the amino and nitro groups. As expected, the amino group is electron-donating and the positive side of the molecular dipole moment (1.59 Debye), while the nitro group is electron-withdrawing and the negative side of the molecular dipole moment (4.92 Debye). Indeed, no matter whether the substituted group is electron-donating or electron-withdrawing, the most affected sites are *ortho* and *para* sites, and there is little change of the electron density on the *meta* positions. These results are in accordance with the rich chemistry literature of physical-organic studies of arene chemistry and our understandings.

Cause of the difference of C–N bonds in aniline and nitrobenzene

The above computations verify that the amino group is electron-donating and the nitro group is electron-withdrawing, and conjugation over the C–N bond always shortens the bond distance. Due to the stronger conjugation in aniline than in nitrobenzene, the C–N bond change is more pronounced in aniline than in nitrobenzene. However, these computations and follow-up analyses do not explain why the C–N bond in nitrobenzene is even longer than in methylamine, particularly, with the deactivation of the conjugation over the C–N bond, the bond distance would be 1.491 and 1.565 Å in aniline and nitrobenzene. In other words, the difference is little changed with or without the conjugation over the C–N bond.

In the valence shell electron pair repulsion (VSEPR) theory,[81,82] lone pair–lone pair repulsion has been well recognized and considered stronger than lone pair–bonding pair repulsion. This can be exemplified by hydrazine (H_2N–NH_2) in three different conformations as shown in Fig. 3. While the N–N

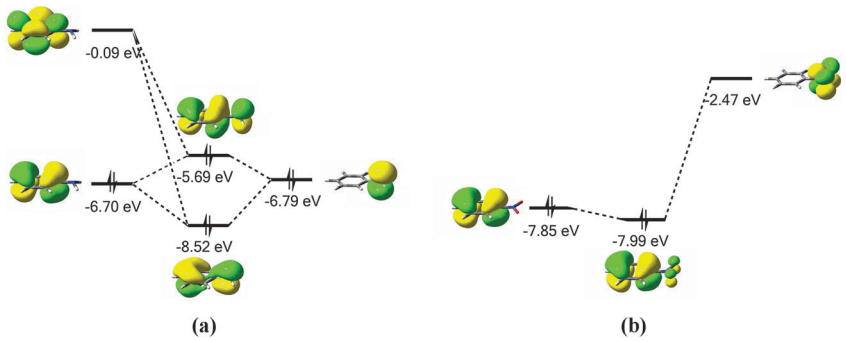

Fig. 1 *"In situ"* orbital interaction diagrams for (a) aniline and (b) nitrobenzene showing the interaction between the benzene ring and substituted amino and nitro groups.

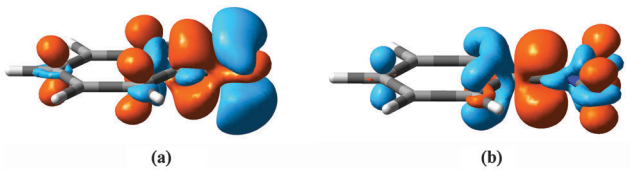

Fig. 2 Electron density difference (EDD) maps showing the conjugation over the C–N bond in aniline (a) and nitrobenzene (b), where the orange color means an increase (gain) of electron density while the cyan color shows a reduction (loss) of electron density.

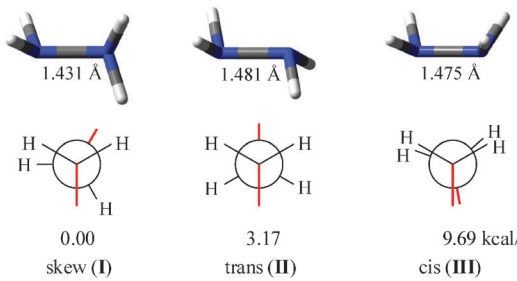

Fig. 3 Comparison of three conformations of hydrazine computed at the B3LYP/6-311+G(d,p) level. The red lines represent the nitrogen lone pairs.

bond in the most stable skew conformer is only 1.431 Å, it is known that the hyperconjugative interaction from the nitrogen lone pairs to the adjacent N–H anti-bonds is the culprit. If the hyperconjugation effect is quenched, the *trans* conformer would be the most stable one.[83] The cis conformer with the N–N bond stretched to 1.475 Å is the transition structure and the least stable one among three conformers, largely due to the strong lone pair–lone pair repulsion. The even longer C–C bond length (1.481 Å) in the *trans* structure results from the enhanced pyramidalization of the nitrogen (the NNH bond angle is 104.5° *versus* 108.8° in **III**), and N eventually uses more p orbital components in the N–N bond with a hybridization mode $sp^{3.56}$ in **II** *versus* $sp^{3.12}$ in **III** based on the natural bond orbital (NBO) analysis.[84,85]

Unlike the much appreciated lone pair–lone pair repulsion, however, a more general π–π repulsion has received less attention so far as the focus for conjugated systems is unanimously on the conjugative stabilization. Most recently, we proposed a new concept, multi-bond strain,[86] to highlight the repulsion among conjugated π bonds or hyperconjugated σ–π bonds in order to settle the argument[87–89] over the claims by Rogers *et al.* that there is no conjugation stabilization in 1,3-butadiyne[90,91] and the conjugation in the cases of 2,3-butanedione and cyanogen is even destabilizing.[92] Using the model systems B_2H_4 and B_4H_2, we quantified the π–π repulsion and showed that it is even stronger than adjacent σ–σ repulsion.[86] This concept of multi-bond strain also elucidates the discrepancy between the experimental (Kistiakowsky[93]) and theoretical (Pauling–Wheland[1,2]) definitions of resonance.

Thus, here we propose that it is the π–π repulsion responsible for the much stretched C–N bond in nitrobenzene compared with aniline. But we note that this π–π repulsion is essentially a kind of steric effect and composed of both Pauli exchange repulsion and electrostatic interaction. To further clarify the cause, we first examined the change of the C–N bond distance with the rotation of the nitro group and all π electrons localized on either the benzene ring or the nitro group (*i.e.*, a BLW computations with three blocks). Indeed, we observed the shortening of the C–N bond in the perpendicular nitrobenzene from 1.565 Å to 1.557 Å (Fig. 4), due to the relief of the π–π Pauli repulsion. But this change is very modest as the π–σ Pauli repulsion comes up in the perpendicular structure, and the energy even goes up by 5.1 kcal mol^{-1} with the diminishing of the stabilizing C–H···O interactions. Considering the delocalization of the lone pair electrons on N to more electronegative oxygen atoms, we speculate that the resonance of the π electrons within the nitro group generates a significant dipole, and the π–π electrostatic

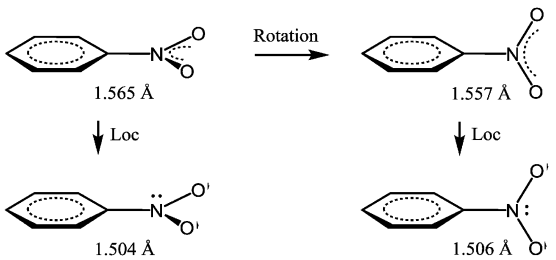

Fig. 4 Variation of the central C–N bond in nitrobenzene with the rotation of the nitro group and the localization of π electrons on the nitro group based on BLW optimizations.

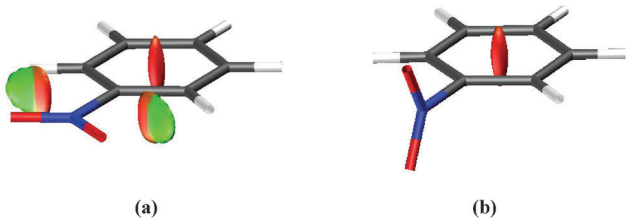

Fig. 5 Gradient isosurfaces with the value of 0.6 a.u. for (a) planar and (b) perpendicular nitrobenzene. The surfaces are colored on a green-red scale (no blue here) according to values of sign(λ_2)ρ, ranging from −0.02 to 0.02 a.u. Green indicates van der Waals attractive interaction, and red indicates steric repulsion. For details see ref. 94 and 95.

repulsion may play a big role in stretching the C–N bond. To prove this hypothesis, we performed BLW optimizations by deactivating the π resonance within the nitro group, and found that there is a significant shortening of the C–N bond in both planar and perpendicular conformations, as shown in Fig. 4. In fact, the values (1.504 and 1.506 Å) are now very much close to the bond distance in aniline (1.491 Å, see Table 2).

To further demonstrate the π–π repulsion within nitrobenzene, we employed the approach developed by Yang and co-workers which can detect and plot noncovalent interactions (NCI) based on the electron density and its reduced gradient.[94,95] It has been shown that the NCI index is related to the QTAIM method.[96] Fig. 5, generated with the Multiwfn program,[97] shows the repulsion between the nitro group and the benzene ring (in red), as well as the attraction between the H and O atoms (in green), in the planar structure. In the perpendicular structure, however, both forces disappear.

The significant electrostatic π–π repulsion may be best justified by the N–N bond in dinitrogen tetroxide (N_2O_4 as shown in Fig. 6), which is very long and very weak.[98,99] Although dinitrogen tetroxide prefers a planar geometry due to the through-space coupling between oxygen atoms rather than the conjugation over the N–N bond which is negligible, the enhanced π–π repulsion stretches the bond to 1.809 Å. By rotating one nitro group around the N–N bond, the central bond is shortened slightly due to the relief of the π–π repulsion, though the cost for the decoupling of O···O interactions is quite high (9.7 kcal mol^{-1}). The deactivation of the π conjugation over the N–N bond stretches the bond to 1.833 Å. Remarkably, if the π conjugation within nitro groups is shut down, the π dipole–dipole electrostatic repulsion would be eliminated, and the N–N bond is significantly shortened to 1.539 Å. The rotation of one nitro group would further relieve the π–π Pauli exchange repulsion and shorten the N–N bond to 1.471 Å, and even more evidently, the perpendicular structure would be more stable than the planar structure by 5.9 kcal mol^{-1}!

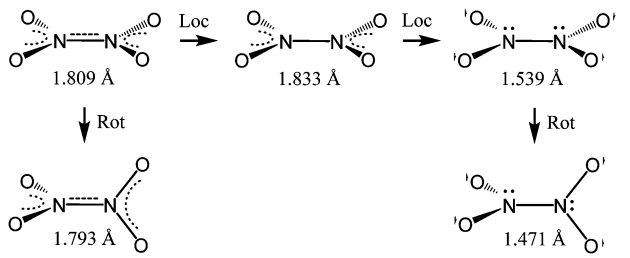

Fig. 6 Evolution of the central N–N bond distance with the gradual localization of π electrons and the rotation of one nitro group based on BLW optimizations.

One may wonder whether the σ induction plays a role as oxygen is highly electronegative. To verify the role of induction for the C–N bond in nitrobenzene, we performed similar computations of dithionitrobenzene as shown in Table 1. It is interesting to note that the NICS values of dithionitrobenzene are very much close to those of aniline rather than those of nitrobenzene, suggesting the enhanced conjugation in dithionitrobenzene than in nitrobenzene. But the replacement of oxygen by sulfur only slightly shortens the C–N bond by 0.009 Å, and slightly enhances the conjugation over the C–N bond, as evidenced by the population analysis (5.923 e in the benzene ring of dithionitrobenzene) and the resonance energies (Table 2). Thus, we conclude that the long C–N bond distance in nitrobenzene as compared to aniline dominantly results from the π effect.

4. Conclusion

Most recently, we proposed the concept of multi-bond strain to recognize the significant π–π repulsion in conjugated systems, as the current view of conjugated systems overemphasizes the conjugation stabilization.[86] The coexistence of stabilizing and repulsive forces in molecules is obvious as the equilibrium geometry of any molecule is a result of the balance of all factors. By recognizing the significant π–π repulsion, it is straightforward to understand the significant difference of the C–N bond distances in aniline and nitrobenzene. In this work, we demonstrated and proved the significant π–π repulsion in nitrobenzene, contributed by both the electrostatic interaction and the Pauli exchange. For comparison, the extremely long and weak N–N bond in N_2O_4 is mainly contributed by the π–π electrostatic repulsion, and the π–π Pauli repulsion plays a secondary but nonnegligible role. The concept of π–π repulsion also explains why the amino group in aniline adopts a pyramidal conformation, though the cost for the planarity is at most only 5 kcal mol^{-1} (a value in ammonia[49]), compared with the much more considerable conjugation energy of 19.3 kcal mol^{-1} (vertical) or 15.2 kcal mol^{-1} (adiabatic). As expected, the conjugation over the C–N bond reduces the aromaticity of the benzene ring, but benefits any substituted benzene as a whole.

Acknowledgements

This work was supported by the US National Science Foundation under the grants CHE-1055310 and CNS-1126438. HZ and XJ acknowledge the financial support from the China Scholarship Council (CSC). WW is grateful for the funding from the National Science Foundation of China (No. 21120102035, 21273176, 21290190).

References

1 L. C. Pauling, *The Nature of the Chemical Bond*, Cornell University Press, Ithaca, NY, 1960.
2 G. W. Wheland, *The Theory of Resonance*, John Wiley & Sons, New York, 1944.
3 P. J. Garratt, *Aromaticity*, Wiley, New York, 1986.
4 V. I. Minkin, M. N. Glukhovtsev and B. Y. Simkin, *Aromaticity and Antiaromaticity: Electronic and Structural Aspects*, Wiley, New York, 1994.
5 P. v. R. Schleyer, *Chem. Rev.*, 2001, **101**, 1115–1118.
6 M. J. S. Dewar and C. De Llano, *J. Am. Chem. Soc.*, 1969, **91**, 789–795.
7 M. J. S. Dewar and G. J. Gleicher, *J. Am. Chem. Soc.*, 1965, **87**, 685–692.
8 B. A. Hess and L. J. Schaad, *J. Am. Chem. Soc.*, 1971, **93**, 305–310.
9 L. J. Schaad and B. A. Hess, *Chem. Rev.*, 2001, **101**, 1465–1476.
10 Y. Mo and P. v. R. Schleyer, *Chem. – Eur. J.*, 2006, **12**, 2009–2020.
11 P. v. R. Schleyer, C. Maerker, A. Dransfeld, H. Jiao and N. J. R. van Eikema Hommes, *J. Am. Chem. Soc.*, 1996, **118**, 6317–6318.
12 Z. Chen, C. S. Wannere, C. Corminboeuf, R. Puchta and P. v. R. Schleyer, *Chem. Rev.*, 2005, **105**, 3842–3888.
13 R. S. Mulliken, *J. Am. Chem. Soc.*, 1952, **74**, 811–824.
14 N. S. Hush, *Trans. Faraday Soc.*, 1961, **57**, 557–580.
15 R. A. Marcus, *Annu. Rev. Phys. Chem.*, 1964, **15**, 155–196.
16 Y. Mo, *J. Chem. Phys.*, 2007, **126**, 224104.
17 Y. Mo, L. Song, M. Liu, Y. Lin, Z. Cao and W. Wu, *J. Chem. Theory Comput.*, 2012, **8**, 800–805.
18 Z. Chen and Y. Mo, *J. Chem. Theory Comput.*, 2013, **9**, 4428–4435.
19 E. Clar, *The Aromatic Sextet*, Wiley, New York, 1972.
20 M. Solà, *Front. Chem.*, 2013, **1**, 22.
21 L. P. Hammett, *Chem. Rev.*, 1935, **17**, 125–136.
22 E. V. Anslyn and D. A. Dougherty, *Modern Physical Organic Chemistry*, University Science Books, Sausalito, CA, 2006.
23 F. A. Carey and R. J. Sundberg, *Advanced Organic Chemistry, Part A: Structure and Mechanisms*, Springer, 2007.
24 M. B. Smith and J. March, *March's Advanced Organic Chemistry: Reactions, Mechanisms, and Structure*, Wiley-Interscience, 2007.
25 R. E. Rawlings, A. K. McKerlie, D. J. Bates, Y. Mo and J. M. Karty, *Eur. J. Org. Chem.*, 2012, 5991–6004.
26 G. Schultz, G. Portalone, F. Ramondo, A. Domenicano and I. Hargittai, *Struct. Chem.*, 1996, **7**, 59–71.
27 A. Domenicano, G. Schultz, I. Hargittai, M. Colapietro, G. Portalone, P. George and C. W. Bock, *Struct. Chem.*, 1990, **1**, 107–122.
28 T. Iijima, H. Jimbo and M. Taguchi, *J. Mol. Struct.*, 1986, **144**, 381–383.
29 A. P. Cox, *J. Mol. Struct.*, 1983, **97**, 61–76.
30 A. A. Zavitsas, *J. Phys. Chem. A*, 2003, **107**, 897–898.
31 S. Blanksby and G. B. Ellison, *Acc. Chem. Res.*, 2003, **36**, 255–263.
32 O. Bludský, J. Šponer, J. Leszczynski, V. Špirko and P. Hobza, *J. Chem. Phys.*, 1996, **105**, 11042–11050.
33 K. P. Sudlow and A. A. Woolf, *J. Chem. Educ.*, 1998, **75**, 108–110.
34 C. W. Bock, P. George and M. a. Tracht, *Theor. Chim. Acta*, 1986, **69**, 235–245.
35 S. Takekiyo, *Mol. Phys.*, 1988, **63**, 407–417.
36 Y. Wang, S. Saebø and C. U. Pittman Jr., *THEOCHEM*, 1993, **281**, 91–98.
37 M. Castellá-Ventura, *Spectrochim. Acta, Part A*, 1994, **50**, 69–86.
38 K. C. Gross and P. G. Seybold, *Int. J. Quantum Chem.*, 2000, **80**, 1107–1115.
39 M. A. Palafox, J. L. Núñez and M. Gil, *THEOCHEM*, 2002, **593**, 101–131.
40 G. M. Roberts, C. A. Williams, J. D. Young, S. Ullrich, M. J. Paterson and V. G. Stavros, *J. Am. Chem. Soc.*, 2012, **134**, 12578–12589.
41 M. Sala, O. M. Kirkby, S. Guérin and H. H. Fielding, *Phys. Chem. Chem. Phys.*, 2014, **16**, 3122–3133.
42 R. Boese, D. Bläser, M. Nussbaumer and T. M. Krygowski, *Struct. Chem.*, 1992, **3**, 363–368.
43 V. A. Shlyapochnikov, L. S. Khaikin, O. E. Grikina, C. W. Bock and L. V. Vilkov, *J. Mol. Struct.*, 1994, **326**, 1–16.
44 S. Irle, T. M. Krygowski, J. E. Niu and W. H. E. Schwarz, *J. Org. Chem.*, 1995, **60**, 6744–6755.
45 O. Exner and T. M. Krygowski, *Chem. Soc. Rev.*, 1996, **25**, 71–75.
46 M. Takezaki, N. Hirota, M. Terazima, H. Sato, T. Nakajima and S. Kato, *J. Phys. Chem. A*, 1997, **101**, 5190–5195.
47 P. C. Chen and S. C. Chen, *Int. J. Quantum Chem.*, 2001, **83**, 332–337.
48 J. C. Sancho-García and A. J. Pérez-Jiménez, *J. Chem. Phys.*, 2003, **119**, 5121–5127.
49 C. Léonard, S. Carter and N. C. Handy, *Chem. Phys. Lett.*, 2003, **370**, 360–365.
50 B. Delley, *J. Chem. Phys.*, 1991, **94**, 7245–7250.
51 *Valence Bond Theory*, ed. D. L. Cooper, Elsevier, Amsterdam, 2002.
52 D. L. Cooper, J. Gerratt and M. Raimondi, *Nature*, 1986, **323**, 699–701.
53 G. A. Gallup, *Valence Bond Methods: Theory and Applications*, Cambridge University Press, New York, 2002.
54 S. S. Shaik and P. C. Hiberty, *A Chemist's Guide to Valence Bond Theory*, Wiley, Hoboken, New Jersey, 2008.
55 W. Wu, P. Su, S. Shaik and P. C. Hiberty, *Chem. Rev.*, 2011, **111**, 7557–7593.
56 Y. Mo, in *The Chemical Bond: Funtamental Apsects of Chemical Bonding*, ed. G. Frenking and S. Shaik, Wiley-VCH, Weinheim, Germany, 2014.
57 Y. Mo and S. D. Peyerimhoff, *J. Chem. Phys.*, 1998, **109**, 1687–1697.
58 Y. Mo, L. Song and Y. Lin, *J. Phys. Chem. A*, 2007, **111**, 8291–8301.
59 Y. Mo, *J. Chem. Phys.*, 2003, **119**, 1300–1306.
60 H. Stoll and H. Preuss, *Theor. Chim. Acta*, 1977, **46**, 11–21.
61 H. Stoll, G. Wagenblast and H. Preuss, *Theor. Chim. Acta*, 1980, **57**, 169–178.

62 E. L. Mehler, *J. Chem. Phys.*, 1977, **67**, 2728–2739.
63 E. L. Mehler, *J. Chem. Phys.*, 1981, **74**, 6298–6306.
64 E. Gianinetti, M. Raimondi and E. Tornaghi, *Int. J. Quantum Chem.*, 1996, **60**, 157–166.
65 E. Gianinetti, I. Vandoni, A. Famulari and M. Raimondi, *Adv. Quantum Chem.*, 1998, **31**, 251–266.
66 A. Famulari, E. Gianinetti, M. Raimondi and M. Sironi, *Int. J. Quantum Chem.*, 1998, **69**, 151–158.
67 R. Z. Khaliullin, E. A. Cobar, R. C. Lochan, A. T. Bell and M. Head-Gordon, *J. Phys. Chem. A*, 2007, **111**, 8753–8765.
68 M. W. Schmidt, K. K. Baldridge, J. A. Boatz, S. T. Elbert, M. S. Gordon, J. J. Jensen, S. Koseki, N. Matsunaga, K. A. Nguyen, S. Su, T. L. Windus, M. Dupuis and J. A. J. Montgomery, *J. Comput. Chem.*, 1993, **14**, 1347–1363.
69 M. J. Frisch, G. W. Trucks, H. B. Schlegel, G. E. Scuseria, M. A. Robb, J. R. Cheeseman, G. Scalmani, V. Barone, B. Mennucci, G. A. Petersson, H. Nakatsuji, M. Caricato, X. Li, H. P. Hratchian, A. F. Izmaylov, J. Bloino, G. Zheng, J. L. Sonnenberg, M. Hada, M. Ehara, K. Toyota, R. Fukuda, J. Hasegawa, M. Ishida, T. Nakajima, Y. Honda, O. Kitao, H. Nakai, T. Vreven, J. A. Montgomery Jr., J. E. Peralta, F. Ogliaro, M. Bearpark, J. J. Heyd, E. Brothers, K. N. Kudin, V. N. Staroverov, T. Keith, R. Kobayashi, J. Normand, K. Raghavachari, A. Rendell, J. C. Burant, S. S. Iyengar, J. Tomasi, M. Cossi, N. Rega, J. M. Millam, M. Klene, J. E. Knox, J. B. Cross, V. Bakken, C. Adamo, J. Jaramillo, R. Gomperts, R. E. Stratmann, O. Yazyev, A. J. Austin, R. Cammi, C. Pomelli, J. W. Ochterski, R. L. Martin, K. Morokuma, V. G. Zakrzewski, G. A. Voth, P. Salvador, J. J. Dannenberg, S. Dapprich, A. D. Daniels, O. Farkas, J. B. Foresman, J. V. Ortiz, J. Cioslowski and D. J. Fox, *Revision C.01*, Gaussian, Inc., Wallingford CT, 2010.
70 T. M. Krygowski, K. Ejsmont, B. T. Stepień, M. K. Cyrański, J. Poater and M. Solà, *J. Org. Chem.*, 2004, **69**, 6634–6640.
71 A. E. Reed, R. B. Weinstock and F. Weinhold, *J. Chem. Phys.*, 1985, **83**, 735–746.
72 F. M. Bickelhaupt and E. J. Baerends, *Angew. Chem., Int. Ed.*, 2003, **42**, 4183–4188.
73 Y. Mo and J. Gao, *Acc. Chem. Res.*, 2007, **40**, 113–119.
74 Y. Mo, W. Wu, L. Song, M. Lin, Q. Zhang and J. Gao, *Angew. Chem., Int. Ed.*, 2004, **43**, 1986–1990.
75 V. Pophristic and L. Goodman, *Nature*, 2001, **411**, 565–568.
76 F. Weinhold, *Angew. Chem., Int. Ed.*, 2003, **42**, 4188–4194.
77 S. Liu, *J. Chem. Phys.*, 2007, **126**, 244103.
78 A. M. Halpern and E. D. Glendening, *J. Chem. Phys.*, 2003, **119**, 11186–11191.
79 P. R. Schreiner, *Angew. Chem., Int. Ed.*, 2002, **41**, 3579–3581.
80 Y. Mo, *Org. Lett.*, 2006, **8**, 535–538.
81 R. J. Gillespie and R. S. Nyholm, *Q. Rev., Chem. Soc.*, 1957, **11**, 339–380.
82 R. J. Gillespie, *Coord. Chem. Rev.*, 2008, **252**, 1315–1327.
83 L. Song, M. Liu, W. Wu, Q. Zhang and Y. Mo, *J. Chem. Theory Comput.*, 2005, **1**, 394–402.
84 A. E. Reed, L. A. Curtiss and F. Weinhold, *Chem. Rev.*, 1988, **88**, 899–926.
85 F. Weinhold and C. Landis, *Valency and Bonding*, Cambridge University Press, Cambridge, England, 2005.
86 Y. Mo, H. Zhang, P. Su, P. D. Jarowski and W. Wu, 2016, to be published.
87 D. Cappel, S. Tüllmann, A. Krapp and G. Frenking, *Angew. Chem., Int. Ed.*, 2005, **44**, 3617–3620.
88 P. D. Jarowski, M. D. Wodrich, C. S. Wannere, P. v. R. Schleyer and K. N. Houk, *J. Am. Chem. Soc.*, 2004, **126**, 15036–15037.
89 F. Feixas, E. Matito, J. Poater and M. Solà, *J. Phys. Chem. A*, 2011, **115**, 13104–13113.
90 D. W. Rogers, N. Matsunaga, A. A. Zavitsas, F. J. McLafferty and J. F. Liebman, *Org. Lett.*, 2003, **5**, 2373–2375.
91 D. W. Rogers, N. Matsunaga, F. J. McLafferty, A. A. Zavitsas and J. F. Liebman, *J. Org. Chem.*, 2004, **69**, 7143–7147.
92 D. W. Rogers, A. Z. Zavitsas and N. Matsunaga, *J. Chem. Educ.*, 2010, **87**, 1357–1359.
93 G. B. Kistiakowsky, J. R. Ruhoff, H. A. Smith and W. E. Vaughan, *J. Am. Chem. Soc.*, 1936, **58**, 146–153.
94 J. Contreras-García, E. R. Johnson, S. Keinan, R. Chaudret, J. P. Piquemal, D. N. Beratan and W. Yang, *J. Chem. Theory Comput.*, 2011, **7**, 625–632.
95 E. R. Johnson, S. Keinan, P. Paula Mori-Sánchez, J. Contreras-García, A. J. Cohen and W. Yang, *J. Am. Chem. Soc.*, 2010, **132**, 6498–6506.
96 J. Contreras-García, W. Yang and E. R. Johnson, *J. Phys. Chem. A*, 2011, **115**, 12983–12990.
97 T. Lu and F. Chen, *J. Comput. Chem.*, 2012, **33**, 580–592.
98 S. S. Wesolowski, J. T. Fermann, T. D. Crawford and H. F. Schaefer III, *J. Chem. Phys.*, 1997, **106**, 7178–7184.
99 R. Ahlrichs and F. Keil, *J. Am. Chem. Soc.*, 1974, **96**, 7615–7620.

